Int. J. Heat Mass Transfer. Vol. 31, No. 1, pp. 91–98, 1988
Printed in Great Britain

0017-9310/88 $3.00+0.00

Combined free–forced convection heat transfer between vertical slender cylinders and power-law fluids

TIAN-YIH WANG and CLEMENT KLEINSTREUER†
Department of Mechanical and Aerospace Engineering, North Carolina State University, Raleigh, NC 27695-7910, U.S.A.

(*Received* 31 *March* 1987 *and in final form* 10 *June* 1987)

Abstract—The transfer processes of steady, laminar mixed convection of non-Newtonian fluids along vertical cylinders are largely determined by the curvature effects of the slender cylinder, the type of thermal boundary conditions, the index of the power-law viscosity model, the buoyancy parameter and the leading edge effect. The validated computer simulation model can be used to investigate basic transport phenomena of the present system and its special cases. The model may also serve as a predictive tool for solving industrial problems related to processing of polymeric liquids.

1. INTRODUCTION

OF FUNDAMENTAL interest in heat and mass transfer are steady temperature and pressure-driven flows of non-Newtonian fluids along cylinders with transverse curvature effect. Applications for such systems can be found in industries processing molten plastics, polymers, food stuff or slurries. Thus considerable attention has been directed towards the analysis and understanding of such problems which are characterized by highly non-linear, coupled partial differential equations. The major components of the system include the heated (or cooled) slender cylinder, the simultaneous free–forced convection heat transfer mechanisms and the power-law fluid.

Previous papers concentrated on one or two of these aspects; predominantly forced convection of polymeric liquids past external surfaces [1–3] or mixed convection from a vertical plate to a power-law fluid [4, 5]. Acrivos *et al.* [1] explored the functional relationship between characteristic groups of this problem (i.e. *Nu* (*Re*, *Pr*), etc.) for very large Prandtl numbers, using inspectional analysis. Kim *et al.* [2] developed universal functions independent of the geometry of two-dimensional or axisymmetric bodies to calculate heat transfer parameters. Recently, Nakayama *et al.* [3] analyzed the same problem using the integral method as a solution technique. Kubair and Pei [4] as well as Lin and Shih [5] employed the local similarity method to study laminar mixed convection heat transfer. Wang and Kleinstreuer [6] presented a new analysis of combined free–forced convection of water at maximum density along a slender, isothermal cylinder.

In this paper all major aspects of the stated convection heat transfer problem are considered. Specifically, a powerful coordinate transformation together with an implicit finite difference method are used to solve the non-similarity problem and to investigate the effects of transverse curvature, power-law index, buoyancy parameter and generalized Prandtl number on the local heat transfer and skin friction coefficients.

2. ANALYSIS

Consider steady laminar axisymmetric boundary-layer flow of a power-law fluid past a vertical slender cylinder at uniform temperature or with a constant surface heat flux. Avoiding wake effects and introducing the Boussinesq assumption, the governing equations read (Fig. 1)

$$\frac{\partial u}{\partial x}+\frac{1}{r}\frac{\partial}{\partial r}(rv)=0 \tag{1}$$

$$u\frac{\partial u}{\partial x}+v\frac{\partial u}{\partial r}=Zg\beta(T-T_\infty)+\frac{K}{\rho r}\frac{\partial}{\partial r}\left(r\left|\frac{\partial u}{\partial r}\right|^{n-1}\frac{\partial u}{\partial r}\right) \tag{2}$$

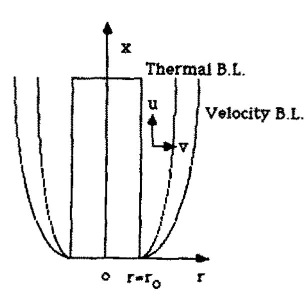

FIG. 1. Schematics of system.

† Author to whom all correspondence should be addressed.

NOMENCLATURE

F	dimensionless stream function
g	gravitational acceleration
Gr	generalized Grashof number
Gr^*	generalized Grashof number
h	local heat transfer coefficient
K	parameter of power-law viscosity model
k	thermal conductivity
L	total length of cylinder
Nu_x	local Nusselt number
n	index for power-law fluid model
Pe	Peclet number
Pr	generalized Prandtl number
Pr_x	generalized local Prandtl number
$\mathbf{q}$	heat flux
Re	generalized Reynolds number (based on r_0)
Re_x	generalized Reynolds number (based on x)
r	radial coordinate
r_0	radius of cylinder
T	temperature
u	velocity component in x-direction
v	velocity component in r-direction
x	longitudinal coordinate
Z	dimensionless parameter, $Z = 1$ for heated cylinders and $Z = -1$ for cooled cylinders.

Greek symbols

α	thermal diffusivity
β	thermal expansion coefficient
ε	transverse curvature parameter
η	pseudo-similarity or combined variable
θ	dimensionless temperature
λ	buoyancy parameter (based on r_0)
λ^*	buoyancy parameter (based on L)
ξ	dimensionless parameter, x/r_0
ξ^*	dimensionless parameter, x/L
ρ	density of fluid
τ	shear stress
ψ	stream function.

Subscripts

∞	ambient condition
q	constant wall heat flux case
T	constant wall temperature case
w	wall condition.

$$u\frac{\partial T}{\partial x}+v\frac{\partial T}{\partial r}=\frac{\alpha}{r}\frac{\partial}{\partial r}\left(r\frac{\partial T}{\partial r}\right). \tag{3}$$

The associated boundary conditions are

$$\text{at } x=0:\ \begin{cases} u=0 \ \text{ and } \ T=T_w \ \text{ when } r=r_0 \\ u=u_\infty \ \text{ and } \ T=T_\infty \ \text{ when } r>r_0 \end{cases}$$

at $r=\infty$: $u=u_\infty$ and $T=T_\infty$;

(i) for the constant wall temperature case

$$T=T_w \ \text{ and } \ u=v=0 \ \text{ at } r=r_0 \tag{4}$$

and

(ii) for the constant wall heat flux case

$$q_w=-k\left.\frac{\partial T}{\partial r}\right|_{r=r_0}. \tag{5}$$

With respect to the mathematical singularity at $x=0$, we assume $u=0$ and $T=T_\infty$ for both cases, the heated cylinder ($Z=1.0$) and the cooled cylinder ($Z=-1.0$).

Now, the following transformation parameters are introduced [6]:

$$\xi=\frac{x}{r_0},\quad \eta=\frac{r^2-r_0^2}{2xr_0}Re_x^{1/(n+1)}$$
$$\psi=r_0u_\infty x\,Re_x^{-1/(n+1)}F(\xi,\eta) \tag{6}$$

with

$$u=\frac{1}{r}\frac{\partial\psi}{\partial r} \quad\text{and}\quad v=-\frac{1}{r}\frac{\partial\psi}{\partial x}$$

$$\theta(\xi,\eta)=\begin{cases}\dfrac{T-T_\infty}{T_w-T_\infty} & \text{for constant surface temperature case} \quad (7a)\\[2ex] \dfrac{T-T_\infty}{\dfrac{q_wx}{k}Re_x^{-1/(n+1)}} & \text{for constant heat flux case} \quad (7b)\end{cases}$$

where n is the flow index, i.e. the key parameter in the power-law viscosity model, and Re_x is the generalized local Reynolds number, defined as

$$Re_x=\frac{\rho u_\infty^{2-n}x^n}{K}.$$

2.1. *The governing equations and parameters for the isothermal surface case*

Transformation of equations (2) and (3), equation (1) is automatically satisfied, yields

$$[(1+\varepsilon\eta)^{(n+1)/2}|F''|^{n-1}F'']'+\frac{1}{n+1}FF''$$
$$=-Z\xi\lambda_T\theta+\xi\left(F'\frac{\partial F}{\partial\xi}-F''\frac{\partial F}{\partial\xi}\right) \tag{8}$$

and

$$\frac{1}{Pr}\xi^{(n-1)/(n+1)}[(1+\varepsilon\eta)\theta']' + \frac{1}{n+1}F\theta' = \xi\left(F'\frac{\partial\theta}{\partial\xi} - \theta'\frac{\partial F}{\partial\xi}\right) \quad (9)$$

where ε is the transverse curvature parameter

$$\varepsilon = 2\left(\frac{\xi}{Re}\right)^{1/(n+1)} \quad \text{with} \quad Re = \rho u_\infty^{2-n} r_0^n/k \quad (10a)$$

Pr is the generalized Prandtl number

$$Pr = \frac{r_0 u_\infty}{\alpha} Re^{-2/(n+1)} \quad (10b)$$

λ_T is the buoyancy parameter

$\lambda_T = Gr\,Re^{-2/(2-n)}$ with

$$Gr = \left(\frac{K}{\rho}\right)^{2/(n-2)} g\beta(T_w - T_\infty) r_0^{(2+n)/(2-n)} \quad (10c)$$

and $Z = 1$ for heated cylinders and $Z = -1$ for cooled cylinders. The corresponding boundary conditions are

$$\text{at } \eta = 0: \quad F(\xi,0) + (n+1)\xi \left.\frac{\partial F}{\partial\xi}\right|_{\eta=0} = 0,$$

$$F'(\xi,0) = 0 \quad \text{and} \quad \theta(\xi,0) = 1$$

$$\text{at } \eta\to\infty: \quad F'(\xi,\infty) = 1 \quad \text{and} \quad \theta(\xi,\infty) = 0. \quad (11a,b)$$

The local skin friction coefficient, defined as

$$c_f = \frac{\tau_w}{\rho u_\infty^2/2} \quad (12a)$$

can now be written as

$$\tfrac{1}{2}c_f Re_x^{1/(n+1)} = [F''(\xi,0)]^n. \quad (12b)$$

The local Nusselt number

$$Nu_x = \frac{hx}{k} = -\frac{\left.\frac{\partial T}{\partial r}\right|_{r=r_0}}{(T_w - T_\infty)/x} \quad (13a)$$

now reads

$$Nu_x Re_x^{-1/(n+1)} = \theta'(\xi,0). \quad (13b)$$

2.2. *The governing equations and parameters for the constant wall heat flux case*

The momentum equation (2) is transformed to

$$[(1+\varepsilon\eta)^{(n+1)/2}|F''|^{n-1}F'']' + \frac{1}{n+1}FF'' = -Z\xi^{(n+2)/(n+1)}\lambda_q\theta + \xi\left(F'\frac{\partial F}{\partial\xi} - F''\frac{\partial F}{\partial\xi}\right) \quad (14)$$

and the energy equation (3) takes on the form

$$\frac{1}{Pr}\xi^{(n-1)/(n+1)}[(1+\varepsilon\eta)\theta']' + \frac{1}{n+1}(F\theta' - F'\theta) = \xi\left(F'\frac{\partial\theta}{\partial\xi} - \theta'\frac{\partial F}{\partial\xi}\right) \quad (15)$$

where the buoyancy parameter

$$\lambda_q = Gr^*\,Re^{-(n+4)/[(n+1)(2-n)]}$$

with

$$Gr^* = \left(\frac{K}{\rho}\right)^{2/(n-2)} g\beta(q_w/k) r_0^{4/(2-n)} \quad (16a)$$

and the local Nusselt number

$$Nu_x Re_x^{-1/(n+1)} = \frac{1}{\theta(\xi,0)}. \quad (16b)$$

The definitions of the other parameters are the same as given in Section 2.1.

The corresponding boundary conditions are

$$\text{at } \eta = 0: \quad F(\xi,0) + (n+1)\xi\left.\frac{\partial F}{\partial\xi}\right|_{\eta=0} = 0,$$

$$F'(\xi,0) = 0 \quad \text{and} \quad \theta'(\xi,0) = -1$$

$$\text{at } \eta\to\infty: \quad F'(\xi,\infty) = 1 \quad \text{and} \quad \theta(\xi,\infty) = 0.$$

3. NUMERICAL ANALYSIS

The transformation of the governing equations, using the method of combined variables [7] reduced the numerical work significantly. To solve this problem with the non-similarity method (cf. ref. [8]) turned out to be too cumbersome. Thus Keller's box method [9], an implicit finite difference scheme, was used. The two-dimensional grid was nonuniform in order to accommodate both, the steep velocity/temperature gradients in the radial direction and the singular point where a fine grid in the streamwise direction was needed near $\xi = 0$. The maximum grid points used for our case studies were 148 ($\xi = 10.0$) in the axial direction and 154 ($\eta = 10.0$) across the boundary layer. The independence of the results from the mesh density has been successfully checked by trial and error.

4. RESULTS AND DISCUSSIONS

Since no measured data sets are available for the system of interest, we reduced the present program to the case of forced convection heat transfer between a vertical plate and a power-law fluid by setting $\lambda_T = 0$ and letting $r_0 \to \infty$, i.e. $\varepsilon = 0$ in equations (8) and (9). Since the radius of transverse curvature is infinite for a flat plate, the reference length r_0 is replaced by L, the test length of the vertical plate. A comparison of our predictive model with previously published results [1, 2] show a good agreement for the skin friction coefficient (cf. Table 1). In Table 2, discrete generalized local Nusselt numbers for dilatant and pseudoplastic fluids subject to mixed convection along a vertical flat plate are compared to results obtained by Lin and Shih [5]. As mentioned earlier (cf. Section 1), they employed the local similarity method which is more accurate when $\xi^* \ll 1$. The starred parameters of Table 2 are based on the plate reference length L replacing the radius r_0.

Tables 3(a) and (b) list typical values of the generalized skin friction coefficient, $[F''(\xi,0)]^n$, and the generalized Nusselt number, $-\theta'(\xi,0)$ or $1/\theta(\xi,0)$, for the present system in the cylinder heating mode. Both system parameters typically increase with increasing buoyancy effects in all power-law fluids. A less uniform behavior can be observed for the generalized local Nusselt number as a function of axial distance when $n > 1.0$ and $\lambda > 0$. This phenomenon is better examined with the following graphs.

Figures 2(a) and (b) show the generalized local Nusselt number or heat transfer grouping (HTG) for various fluids characterized by different Prandtl numbers and power-law indices. For both thermal boundary conditions, HTG $= Nu_x/Re^{1/(n+1)}$ attains larger values with higher Prandtl numbers for all types of fluids and it increases monotonously along the cylinder axis for pseudoplastic and Newtonian fluids.

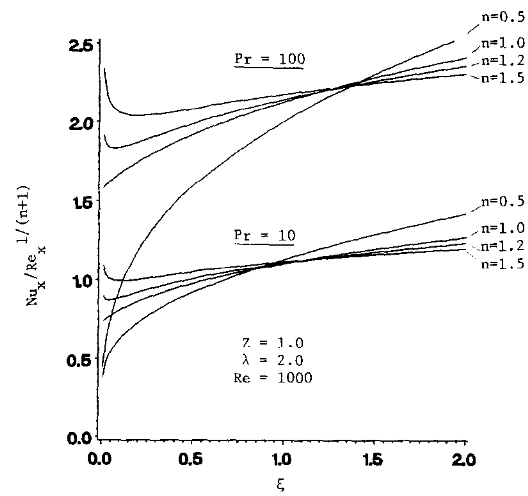

FIG. 2(a). Local Nusselt number for different fluids along a heated isothermal cylinder.

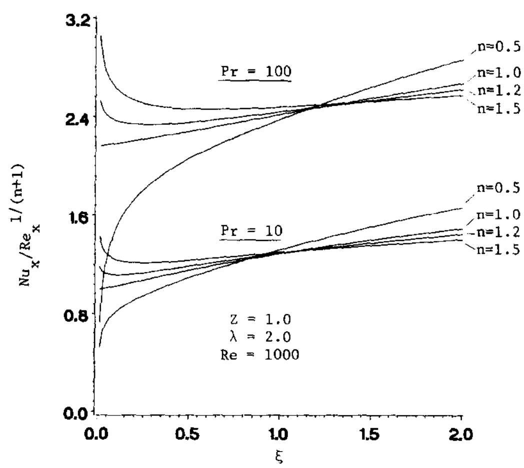

FIG. 2(b). Local Nusselt number for different fluids along a heated cylinder with constant surface heat flux condition.

Table 1. Comparison of local skin friction coefficient c_f (equation (12b)) for forced convection heat transfer from a vertical plate to power-law fluids

n	Acrivos *et al.* [1]	Kim *et al.* [2]	$\xi^* = x/L$	Present method
0.5	0.5755	—	0.1	0.5786
			1.0	0.5785
1.0	0.3320	—	0.1	0.3320
			1.0	0.3320
1.2	0.2750	0.2780	0.1	0.2780
			1.0	0.2780
1.5	0.2189	—	0.1	0.2204
			1.0	0.2204
2.0	0.1612	0.1598	0.1	0.1600
			1.0	0.1598

However, for dilatant fluids ($n > 1.0$) the local HTG reduces very rapidly from a high value near $\xi = 0$, exhibits somewhat of a minimum at small ξ and then increases slightly thereafter. The trend is the same for

Table 2. Comparison of local Nusselt numbers for the power-law fluids along vertical plates subjected to (a) constant wall temperature condition and (b) constant wall heat flux condition; $Pr = 10$

		$\lambda^* = 0$				$\lambda^* = 1.0$				$\lambda^* = 2.0$			
		Lin and Shih [5]		Present method		Lin and Shih [5]		Present method		Lin and Shih [5]		Present method	
n	ξ^*	$T_w =$ const.	$q_w =$ const.	$T_w =$ const.	$q_w =$ const.	$T_w =$ const.	$q_w =$ const.	$T_w =$ const.	$q_w =$ const.	$T_w =$ const.	$q_w =$ const.	$T_w =$ const.	$q_w =$ const.
0.5	0.01	0.4781	0.6551	0.4776	0.6260	0.6648	0.9210	0.6671	0.9135	0.7656	1.0429	0.7684	1.0306
	0.1	0.6183	0.8485	0.6202	0.8323	0.8419	1.1138	0.8458	1.0774	0.9753	1.2519	0.9771	1.2206
	1.0	0.8007	1.0975	0.8031	1.0190	1.0570	1.3512	1.0623	1.2592	1.2205	1.4995	1.2228	1.4192
1.5	0.01	0.9493	1.3002	1.0725	1.4151	1.1417	1.4808	1.1954	1.5834	1.2437	1.5800	1.2710	1.6405
	0.1	0.8137	1.1148	0.8994	1.1962	0.9937	1.3028	1.0323	1.3755	1.0858	1.3982	1.1097	1.4703
	1.0	0.6973	0.9557	0.7683	1.0241	0.8646	1.1486	0.9243	1.2129	0.9475	1.2390	1.0069	1.3040

Table 3(a). Typical values of generalized skin friction coefficient and Nusselt number for power-law fluids along heated, isothermal cylinders with different buoyancy effects; $Re = 1000$ and $Pr = 100$

		$[F''(\xi,0)]^n$			$-\theta'(\xi,0)$		
n	ξ	$\lambda_T = 0.0$	$\lambda_T = 1.0$	$\lambda_T = 2.0$	$\lambda_T = 0.0$	$\lambda_T = 1.0$	$\lambda_T = 2.0$
0.5	0.01	0.5104	0.5199	0.5291	0.4321	0.4373	0.4424
	0.1	0.5150	0.5707	0.6218	0.8414	0.8921	0.9375
	1.0	0.5252	0.8306	1.0636	1.3875	1.7569	2.0057
	2.0	0.5325	1.0384	1.3976	1.5483	2.1754	2.5498
1.5	0.01	0.2264	0.2289	0.2315	2.3281	2.3331	2.3380
	0.1	0.2315	0.2595	0.2865	1.9753	2.0182	2.0568
	1.0	0.2475	0.5307	0.7741	1.7359	2.0127	2.1759
	2.0	0.2556	0.7976	1.2462	1.6805	2.1013	2.3093

Table 3(b). Typical values of generalized skin friction coefficient and Nusselt number for power-law fluids along heated, constant wall heat flux cylinders with different buoyancy effects; $Re = 1000$ and $Pr = 100$

		$[F''(\xi,0)]^n$			$1/\theta(\xi,0)$		
n	ξ	$\lambda_q = 0.0$	$\lambda_q = 1.0$	$\lambda_q = 2.0$	$\lambda_q = 0.0$	$\lambda_q = 1.0$	$\lambda_q = 2.0$
0.5	0.01	0.5104	0.5111	0.5117	0.7241	0.7243	0.7246
	0.1	0.5150	0.5216	0.5280	1.4837	1.4893	1.4948
	1.0	0.5252	0.6386	0.7315	2.1307	2.2712	2.3819
	2.0	0.5325	0.7959	0.9808	2.3050	2.6442	2.8637
1.5	0.01	0.2264	0.2265	0.2266	3.0661	3.0663	3.0665
	0.1	0.2315	0.2351	0.2387	2.6142	2.6193	2.6243
	1.0	0.2475	0.3550	0.4485	2.2861	2.3974	2.4796
	2.0	0.2556	0.5269	0.7420	2.2060	2.4389	2.5760

higher Prandtl numbers which are typical for certain polymeric liquids. This behavior is quite different when compared to the vertical flat plate configuration [4, 5]. There, $Nu_x Re_x^{-1/(n+1)}$ decreases from the leading edge downstream for dilatant fluids and increases for pseudoplastics towards a constant value for a given Newtonian fluid. The reason for the different behavior is the transverse curvature effect which, in terms of the parameter ε, varies with x and n. The significantly different behavior of the two power-law fluids near $\xi = x/r_0 = 0$ can be explained as follows. Mathematically, for $x \to 0$, the coefficient of the highest derivative in the energy equation (equation (9) or (15)), is dominant for pseudoplastics and very small for dilatant fluids.

Specifically

$$\frac{1}{Pr}\left(\frac{x}{r_0}\right)^{(n-1)/(n+1)} \begin{cases} \to \infty & \text{for } n < 1 \\ \to 0 & \text{for } n > 1 \end{cases}$$

which implies that different values for $\theta'(\xi, 0) \propto$ HTG are generated (cf. Figs. 4(a)–(c) and 6(a) and (b)). On

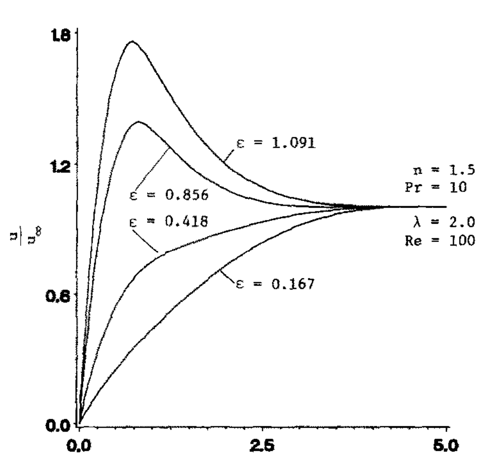

FIG. 3. Transverse curvature effect of heated isothermal cylinders on velocity profiles for dilatant fluids ($n > 1.0$).

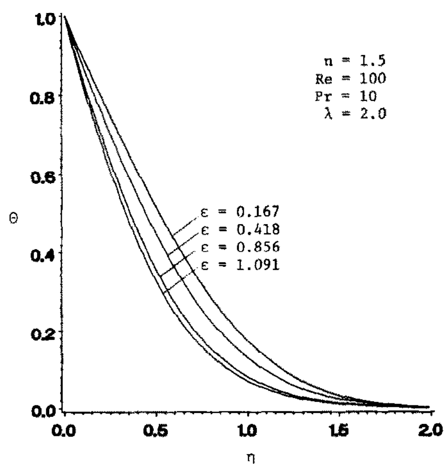

FIG. 4(a). Transverse curvature effect of heated isothermal cylinders on temperature profiles for dilatant fluids ($n > 1.0$) at $Re = 100$.

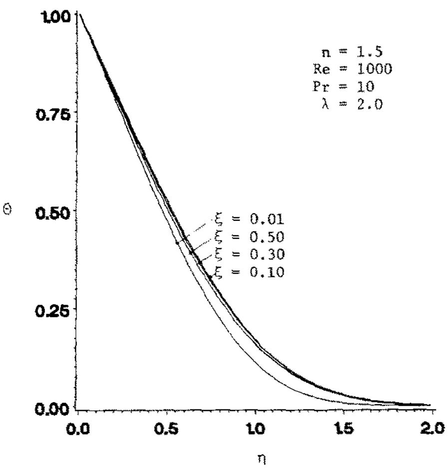

FIG. 4(b). Transverse curvature effect of heated isothermal cylinders on temperature profiles for dilatant fluids ($n > 1.0$) at $Re = 1000$.

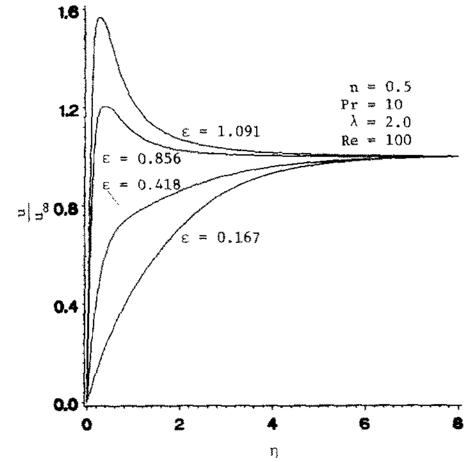

FIG. 5. Transverse curvature effect of heated cylinders on velocity profiles for pseudoplastics ($n = 0.5$).

a more physical note, one could rewrite this coefficient in the form of a generalized local Prandtl number, namely, for $x \to 0$

$$Pr_x = Pr\left(\frac{x}{r_0}\right)^{(1-n)/(n+1)} \begin{cases} \to \infty & \text{for } n > 1 \\ \to 0 & \text{for } n < 1. \end{cases}$$

Noting that $\mathrm{HTG} \equiv Nu_x/Re_x^{1/(1+n)}$ is governed by $Pr_x \sim \delta/\delta_{th}$, we can expect that the magnitude of HTG near the leading edge is very high for dilatant fluids and low for pseudoplastics. As ξ increases, the difference reduces quickly and at certain ξ-values, for a given Prandtl number, the HTG numbers for pseudoplastics exceed those of dilatant fluids. For the comparable vertical plate system, the HTGs for both power-law fluids seem to approach asymptotically the constant HTG value for the equivalent Newtonian fluid.

Figures 3–6 depict the effects of transverse curvature and power-law index on the velocity and tem-

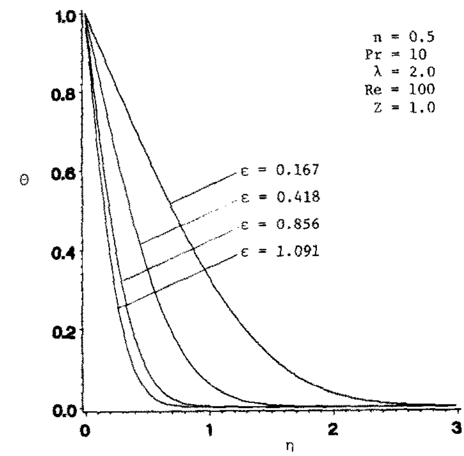

FIG. 6(a). Transverse curvature effect of heated cylinders on temperature profiles for pseudoplastics ($n = 0.5$) at $Re = 100$.

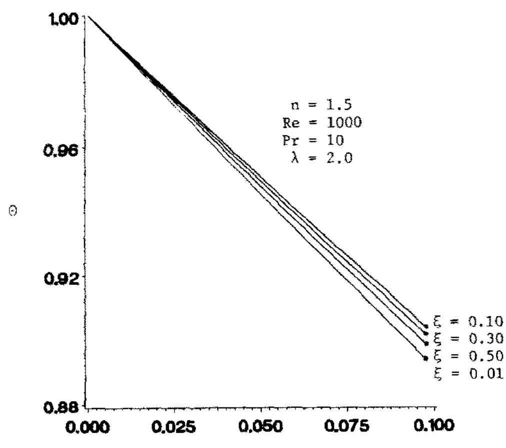

FIG. 4(c). Transverse curvature effect of heated isothermal cylinders on temperature profiles for dilatant fluids ($n > 1.0$) at $Re = 1000$; enlarged near $\xi = 0$.

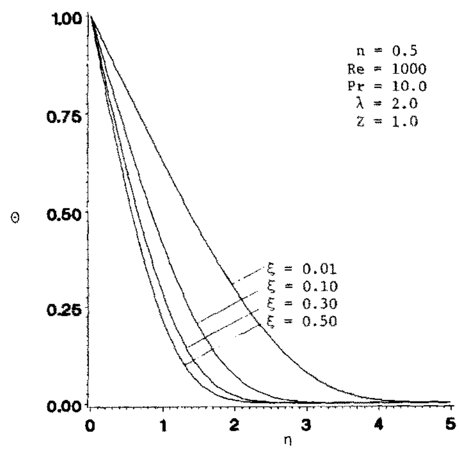

FIG. 6(b). Transverse curvature effect of heated cylinders on temperature profiles for pseudoplastics ($n = 0.5$) at $Re = 1000$.

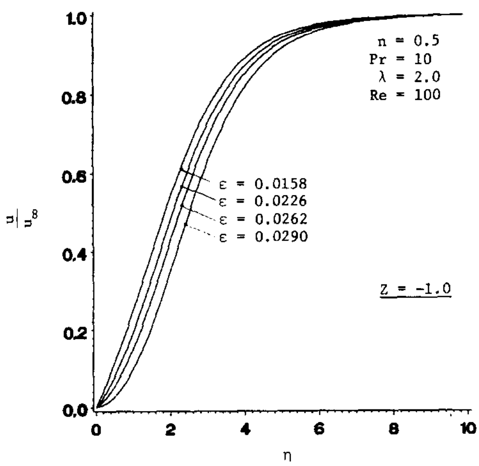

FIG. 7. Transverse curvature effect of cooled cylinders on velocity profiles for pseudoplastics ($n = 0.5$).

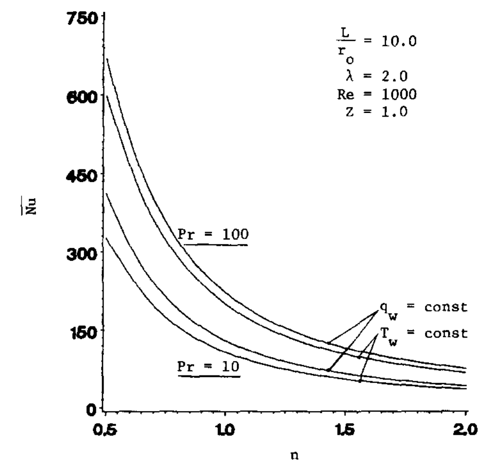

FIG. 8. Average Nusselt number as a function of power-law index n and generalized Prandtl number Pr.

perature profiles for polymeric liquids. A rather low thermal Peclet number, $Pe = Pr\,Re$, was selected for the velocity graphs in order to demonstrate with Figs. 3 and 5 the strong interaction between the buoyancy force and the effect of transverse curvature. Larger ε's ($\varepsilon > 0.5$) act as favorable pressure gradients and hence cause a velocity overshoot when compared with pure forced convection flow past a heated surface. In contrast, for mixed convection flow past a cooled cylinder (cf. Fig. 7), an increase of ε will produce an adverse pressure gradient, i.e. the buoyancy force tends to retard the forced convection flow and flow separation may occur (cf. Fig. 7, curve $\varepsilon = 0.029$ near $\eta = 0$). At higher Prandtl or Peclet numbers the overshoot diminishes since viscous effects become so much larger than thermal diffusion. The temperature profiles for dilatant fluids (Figs. 4(a)–(c)) and pseudoplastics (Figs. 6(a) and (b)) are directly related to the unusual behavior of the local heat transfer grouping for the two types of polymeric liquids in the vicinity of the leading edge. An increase in the freestream Reynolds number basically reduces the curvature effect for dilatant fluids (Figs. 4(a) and (b)) and increases the thermal boundary-layer thickness for pseudoplastics (Figs. 6(a) and (b)). Figure 4(c) depicts the enlarged temperature gradient along the cylinder surface in support of the unique behavior of the HTG for dilatant fluids.

Figure 8 shows the average Nusselt number as a function of the power-law index, n, for different generalized Prandtl numbers and thermal boundary conditions.

REFERENCES

1. A. M. Acrivos, J. J. Shah and E. E. Peterson, Momentum and heat transfer in laminar boundary layer flow of non-Newtonian fluids past external surface, *A.I.Ch.E. Jl* **6**, 312–317 (1960).
2. H. W. Kim, D. R. Jeng and K. J. Dewitt, Momentum and heat transfer in power-law fluid flow over two-dimensional or axisymmetric bodies, *Int. J. Heat Mass Transfer* **26**, 245–259 (1983).
3. A. Nakayama, A. V. Shenoy and H. Koyama, An analysis for forced convection heat transfer from external surfaces to non-Newtonian fluids, *Wärme- und Stoffübertr.* **20**, 219–227 (1986).
4. V. G. Kubair and D. C. Pei, Combined laminar free and forced heat transfer to non-Newtonian fluids, *Int. J. Heat Mass Transfer* **11**, 855–868 (1968).
5. H. T. Lin and Y. P. Shih, Combined laminar free and forced convection from a vertical plate to power law fluids, *Chem. Engng Commun.* **7**, 327–334 (1980).
6. T.-Y. Wang and C. Kleinstreuer, Natural and combined free–forced convection boundary-layer flow of water at 4°C on vertical slender cylinders, *J. Thermophys. Heat Transfer* (1988), in press.
7. C. Kleinstreuer, *Engineering Fluid Dynamics—An Interdisciplinary Systems Approach*. Springer, New York (1988/89), to be published.
8. J.-Y. Liu, W. J. Minkowycz and P. Cheng, Conjugated, mixed convection–conduction heat transfer along a cylinder fin in a porous medium, *Int. J. Heat Mass Transfer* **29**, 769–775 (1986).
9. T. Cebeci and P. Bradshaw, *Momentum Transfer in Boundary Layers*. Hemisphere, Washington, D.C. (1977).

CONVECTION THERMIQUE ENTRE DES CYLINDRES VERTICAUX ET DES FLUIDES A LOI-PUISSANCE

Résumé—Les mécanismes de transfert de la convection laminaire, mixte, permanente des fluides non newtoniens le long des cylindres verticaux sont largement conditionnés par les effets de courbure du cylindre mince, du type de condition limite thermique, de l'indice du modèle de viscosité en loi-puissance, du paramètre de flottement et par l'effet de bord d'attaque. Le modèle de simulation numérique peut être utilisé pour étudier les phénomènes de transfert dans le système considéré et leurs cas particuliers. Le modèle peut aussi servir comme un outil prédictif pour résoudre des problèmes industriels relatifs aux polymères liquides.

DER WÄRMEÜBERGANG DURCH MISCH-KONVEKTION ZWISCHEN VERTIKALEN; SCHLANKEN ZYLINDERN UND POWER-LAW-FLUIDEN

Zusammenfassung—Der Vorgang der Wärmeübertragung bei stationärer laminarer Mischkonvektion von nicht-newton'schen Fluiden entlang vertikaler Zylinder sind größtenteils bestimmt durch die Krümmungseffekte der schlanken Zylinder, die Art der thermischen Randbedingungen, den Index des Potenz-Ansatzes für das Viskositäts-Modell, den Auftriebsparameter und Einflüsse durch die Anströmkante. Das gesicherte Simulationsmodell kann zur Erforschung von grundlegenden Transport-Phänomenen und Spezialfällen des vorliegenden Systems benutzt werden. Das Modell kann ebenso zur Lösung industrieller Probleme dienen, die bei der Verarbeitung polymerer Flüssigkeiten auftreten.

СЛОЖНЫЙ ТЕПЛООБМЕН ЕСТЕСТВЕННОЙ И ВЫНУЖДЕННОЙ КОНВЕКЦИЕЙ МЕЖДУ ВЕРТИКАЛЬНЫМИ УЗКИМИ ЦИЛИНДРАМИ И СТЕПЕННЫМИ ЖИДКОСТЯМИ

Аннотация—Процессы переноса стационарной ламинарной смешанной конвекцией неньютоновских жидкостей вдоль вертикальных цилиндров определяются, главным образом, кривизной узкого цилиндра, типом тепловых граничных условий, показателем степенного закона, принятого для вязкости, параметром плавучести и влиянием передней кромки. Для исследования основных явлений переноса в данной системе и частных случаев можно использовать машинное моделирование, которое может также применяться для решения технических задач производства полимерных жидкостей.